2020

Geostatistical features of streambed vertical hydraulic conductivities in Frenchman Creek Watershed in Western Nebraska

Olufemi P. Abimbola

Aaron R. Mittelstet

Troy E. Gilmore

Geostatistical features of streambed vertical hydraulic conductivities in Frenchman Creek Watershed in Western Nebraska

Olufemi P. Abimbola,[1] Aaron R. Mittelstet,[1] & Troy E. Gilmore[1,2]

1 Department of Biological Systems Engineering, University of Nebraska-Lincoln, Lincoln, Nebraska
2 Conservation and Survey Division, School of Natural Resources, University of Nebraska-Lincoln, Lincoln, Nebraska

Correspondence: Aaron R. Mittelstet, Department of Biological Systems Engineering, University of Nebraska- Lincoln, 223 L. W. Chase Hall, Lincoln, NE 68583-0726.
Email: amittelstet2@unl.edu

ORCID Aaron R. Mittelstet https://orcid.org/0000-0001-9857-5539

Abstract

This study evaluated the spatial variability of streambed vertical hydraulic conductivity (K_v) in different stream morphologies in the Frenchman Creek Watershed, Western Nebraska, using different variogram models. Streambed K_v values were determined in situ using permeameter tests at 10 sites in Frenchman, Stinking Water and Spring Creeks during the dry season at baseflow conditions. Measurements were taken both in straight and meandering stream channels during a 5 day period at similar flow conditions. Each test site comprised of at least three transects and each transect comprised of at least three K_v measurements. Linear, Gaussian, exponential

Published in *Hydrological Processes.* 2020;1–11.
DOI: 10.1002/hyp.13823

Submitted 8 August 2019; Accepted 15 May 2020.

and spherical variogram models were used with Kriging gridding method for the 10 sites. As a goodness-of-fit statistic for the variogram models, cross-validation results showed differences in the median absolute deviation and the standard deviation of the cross-validation residuals. Results show that using the geometric means of the 10 sites for gridding performs better than using either all the K_v values from the 93 permeameter tests or 10 K_v values from the middle transects and center permeameters. Incorporating both the spatial variability and the uncertainty involved in the measurement at a reach segment can yield more accurate grid results that can be useful in calibrating K_v at watershed or sub-watershed scales in distributed hydrological models.

Keywords: Frenchman Creek, geostatistical analysis, permeameter test, streambed, variogram models, vertical hydraulic conductivity

1 Introduction

There is a broad interest in the estimation of streambed vertical hydraulic conductivity (K_v) due to its connection to water quality, aquatic habitat, and groundwater-surface water exchange (Cheng, Song, Chen, & Wang, 2011; Genereux, Leahy, Mitasova, Kennedy, & Corbett, 2008; Jiang et al., 2015; Wang et al., 2017). Streams are rarely isolated. The different states of connection between streams and underlying groundwater, and the water exchange pattern at the groundwater-surface water interface are mostly dependent on rainfall inputs, water head changes, and substrate permeability (Brunner, Cook, & Simmons, 2009; Castro & Hornberger, 1991). There are variations in K_v values in a watershed due to hydrologic position and scale (Katsuyama, Tani, & Nishimoto, 2010), as well as the variety of spatial and temporal factors such as the topography, the depth of streambed, bed slope, land cover, and the hydrogeological setting of the underlying aquifer (Wang et al., 2016;Woessner, 2000).

Streambed K_v is a key parameter in watershed models, so understanding its spatial variability and uncertainty is essential to accurately predict how stresses and environmental signals propagate through the hydrologic system (Abimbola, Mittelstet, Gilmore, & Korus, 2020). In situ studies have shown that streambed K_v changes significantly along the stream or river cross section (perpendicular to the streamflow) and along the stream flow (in the downstream direction), even in a small channel segment (Chen, 2004, 2005; Cheng et al., 2011; Genereux et al., 2008; Hatch, Fisher, Ruehl, & Stemler, 2010). Since it is not practical to measure K_v at every location along a stream course,

most hydrological modelling studies usually assume homogeneity of K_v for practical reasons. Relying on literature values or limited measurements and assuming K_v is constant across a watershed may lead to more uncertainty due to the under- or over-prediction of streambed leakage and baseflow (Brunner et al., 2009; Irvine, Brunner, Franssen, & Simmons, 2012; Kurtz, Hendricks Franssen, Brunner, & Vereecken, 2013; Leake, Greer, Watt, & Weghorst, 2008). To understand the connectivity between surface water and groundwater, it is important to estimate the spatial distribution of K_v which is one of the most important parameters controlling the movement of water from the stream to the aquifer, and vice versa (Chen & Shu, 2002; Genereux et al., 2008; Goswami, Kalita, & Mehnert, 2010; Saenger, Kitanidis, & Street, 2005; Sun & Zhan, 2007).

Several studies have found ways to measure K_v in situ (Chen, 2005, 2007; Genereux et al., 2008) mostly building on Hvorslev (1951). While some studies focused on the spatial variability of streambed K_v along transects across a channel (Cardenas & Zlotnik, 2003; Chen, 2004; Kennedy, Genereux, Mitasova, Corbett, & Leahy, 2008), others focused on both the spatial and temporal variability (Genereux et al., 2008), as well as statistical description of streambed K_v (Cardenas & Zlotnik, 2003; Song, Chen, Cheng, Summerside, & Wen, 2007). Although most of the previous studies focused on the spatial variability of streambed K_v at one or several adjacent sites in small creeks and at distant sites along large rivers (Cardenas & Zlotnik, 2003; Chen, 2005; Cheng et al., 2011; Genereux et al., 2008; Song et al., 2007), they did not develop a geostatistical distribution analysis of streambed K_v across multiple stream orders at watershed-scale. Few studies have quantified the spatial variability of K_v in different stream morphologies, and very few have considered using different variogram models (Jiang et al., 2015; Wang et al., 2017). These geostatistical methods of estimating K_v suggest challenges in determining representative samples and comparing results, considering the heterogeneity and anisotropy of streambed materials and geological conditions (Naganna, Deka, Sudheer, & Hansen, 2017). Moreover, although geostatistical methods present a wide range of interpolation procedures that can be applied to hydrological systems, there is a knowledge gap in incorporating interpolation results into hydrological modelling for better calibration.

In the past 25 years, there have been significant changes in water resources in Western Nebraska. This includes increases in irrigated

acres and irrigation wells; decreases in streamflow, groundwater levels, and groundwater allocations; conversion from flood to pivot irrigation technologies and drip irrigation; moratoriums on new irrigation wells; and the encroachment of the eastern Red Cedar and other invasive species (Twidwell et al., 2013). The Frenchman Creek Watershed in Nebraska has experienced each of these changes. In the last five decades, groundwater withdrawals in the Frenchman Creek Watershed have led to groundwater declines ranging from 2 to 17 m and decreased streamflow. In the 1960s, Frenchman Creek began several kilometers west of the Colorado border, yet today it begins 21 km east of the Colorado border (Traylor, 2012). These declines have led to reductions in groundwater allocations and a moratorium on new irrigation wells in the Upper Republican River Natural Resource District (NRD). Since K_v is a major parameter in the estimation of groundwater recharge from streams and rivers, it is therefore important to determine its spatial distribution for integrated water resource assessment and management in the watershed.

The objectives of this study were to (a) determine the statistical distribution and spatial variation of streambed K_v along different morphologies within the Frenchman Creek Watershed and (b) evaluate the accuracy and usefulness of the spatial variability of streambed K_v values as estimated from different sample sizes and using different representative samples.

2 Materials and methods

2.1 Study area and test sites

The Frenchman Creek Watershed is located in two states (Nebraska and Colorado) in the United States. The watershed drains over 7,600 km^2 in southwest Nebraska (60%) and southeast Colorado (40%; Figure 1). It is a sub-watershed of the Republican River watershed. The primary land uses in the watershed consist of irrigated cropland, dry cropland, pasture, and rangeland, with dense vegetation including trees, shrubs, and grasses occurring in the riparian zones. The dominant soil series include Valent (70–100% sand) and Kuma (19–79% silt), and major tributaries include Stinking Water Creek, Spring Creek, and Sand Creek.

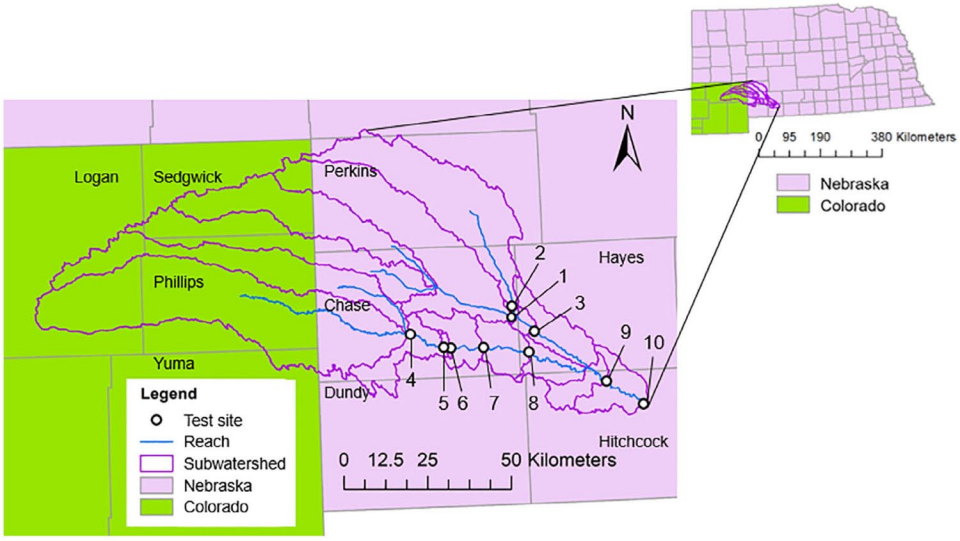

Figure 1 Map showing the 10 sites and sub watersheds where in situ permeameter tests were performed in the Frenchman Creek Watershed.

Ten test sites (stream reaches) were selected from third-, fourth-, and fifth-order streams on the Frenchman Creek and its four main tributaries (Figure 2). The sites were selected above and below the major confluences, and were located in both meandering and straight reaches. The number of sites was constrained due to stream accessibility and streamflow. The western two thirds of the watershed was dry.

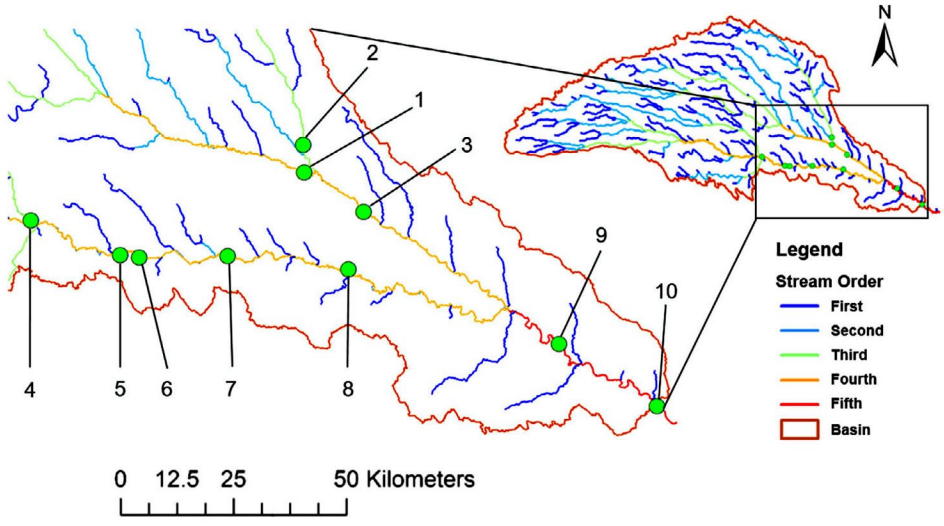

Figure 2 Stream orders of the measurement sites.

Figure 3 Basic design of falling-head permeameter test. *Left*: Schematic of the field permeameter. *Middle*: Photograph of permeameters with each tube installed to depth of 30 cm. *Right*: Layout of three transects along the stream for each site.

2.2 In situ permeameter tests

The in situ falling head permeameter test is one of several methods used to determine streambed K_v (Chen, 2000; Dong, Chen, Wang, Ou, & Liu, 2012; Genereux et al., 2008). The falling head permeameter test usually involves inserting a tube into channel sediments (Figure 3). In this study, transparent tubes were used for 10 test sites within the Frenchman Creek Watershed in the summer of 2017. Seven sites were on Frenchman Creek, two sites are on Stinking Water Creek and one site on Spring Creek. Other tributaries within the watershed were dry at the time of the study. Field measurements were carried out over a 5-day period from June 26th to 30th, 2017. The stream was at baseflow conditions with average discharge of 0.35 $m^3\ s^{-1}$ at the USGS gage station near Palisade (06834000). The flow remained consistent throughout the study period with a flowrate on June 26th of 0.36 $m^3\ s^{-1}$ and decreasing slightly to 0.33 $m^3\ s^{-1}$ by June 30th. This compares to an average discharge at the Palisade gage station of 0.65 $m^3\ s^{-1}$ from 2000 to 2020.

The duration of individual falling head tests ranged from a few minutes to a maximum of 24 hours. Permeameters left for long periods of time were covered with plastic bags to prevent evaporative losses.

Each test site comprised of at least three transects and each transect comprised of at least three streambed K_v measurements. Figure 3 is a schematic diagram showing in situ permeameter test installation at a test site. Transparent tubes (76 cm long and 8 cm inside diameter

or 183 cm long and 6.8 cm inside diameter) were pressed vertically into the channel sediments. The thickness of the tube wall was about 3 mm, typical of many previous studies (Genereux et al., 2008; Kennedy et al., 2008). For each K_v measurement, the tube was pressed to a depth of 30 cm, thus the lower part of the tube was filled with a sediment column of 30-cm length (Song et al., 2018). Stream water level was used as an estimate of the ambient pre-test water level, which introduces additional error in the K_v estimates (compared to Genereux et al., 2008, where groundwater head was measured) but that error is in most cases small relative to the order of magnitude differences in K_v observed between sites in this study. Clear stream water was then added slowly to fill up the tube from the top, minimizing the disturbance of sediment inside the tube. As the hydraulic head in the tube began to fall, a series of hydraulic heads at given times were recorded. Three (low conductivity) to ten (high conductivity) measurements were recorded for each test. The K_v (m/d) calculation was based on Equation (1) derived from Hvorslev's equation, similar to Genereux et al. (2008).

$$K_v = \frac{\frac{\pi D}{11m} + L_v}{(t_2 - t_1)} \ln\left(\frac{H_1}{H_2}\right)$$

where D is the inside diameter of the tube; L_v is the length of the sediment in the tube; t_1 and t_2 are the times between inside measurements of hydraulic heads H_1 and H_2, respectively; and m is the isotropic transformation ratio $(K_h/K_v)^{½}$ where K_h is the horizontal hydraulic conductivity of the sediment around the base of the tube. For this study, we used the average of the K_v values estimated with $m = 1$ and $m = \infty$. If t_1 is the time of the start of the permeameter test (i.e., $H_1 = H_0$ at $t_1 = 0$), Equation (1) gives Equation (2)

$$\ln H = -\frac{K_v}{\frac{\pi D}{11m} + L_v} t + \ln H_0$$

where H is the water level inside the permeameter relative to the ambient pre-test water level, and t is time, and the slope term is set equal to the slope in the head versus time plot and solved for K_v (Genereux et al., 2008).

2.3 Normality test

To check whether the distributions of K_v were normal for the sites, graphical exploration (Q–Q plots and histograms) and formal tests of normality were carried out. There are quite a number of tests of normality available in the literature. D'Agostino and Stephens (1986) provided detailed descriptions of various normality tests. In this study, six normality tests were used. Anderson–Darling (AD), Cramer–von Mises (CVM), Lilliefors (LL), Pearson chi-square (CSQ), Shapiro– Francia (SF), and Shapiro–Wilk (SW) tests were applied at .05 significance level. These normality tests were categorized into tests based on correlation and regression (SW and SF tests), CSQ test, and empirical distribution test (such as LL, AD, and CVM). Some of these tests were constructed to be applied under certain conditions or assumptions. The SW (Shapiro & Wilk, 1965) test is one of the most commonly used of the six tests. According to Royston (1982), it has requirements for the sample size N ($7 \leq N \leq 2{,}000$), while the LL (Lilliefors, 1967) test is preferable to apply for a large sample size $N \geq 2{,}000$ (Cheng et al., 2011). The SF test is a simplified version of the SW test, which uses the squared normal probability plot correlation as a test statistic.

2.4 Gridding streambed K_v

For each site (stream reach), the spatial structure of K_v was analysed and different variograms were fit to the data and used as input in the software package SURFER (http://www.GoldenSoftware.com). Spatial interpolation of the K_v data was carried out using kriging. Kriging, which is the most commonly used geostatistical method, can estimate both the predicted values and their standard errors (Webster & Oliver, 2001). It is also an optimal interpolator which uses the spatial structure and variance of the input data points to estimate the interpolation weights and search radii to provide the best, unbiased estimate at unsampled points (Burrough & McDonnell, 1998).

The performance of kriging depends on the presence of spatial autocorrelation. This implies that sites which are close together tend to be more similar than those which are further apart. Since K_v values may vary in orders of magnitude within a short distance in a heterogeneous aquifer system, the geometric mean of each site was used in

this study to capture the variations. Variograms were created from the input K_v data points by plotting the variance against the distance between pairs of points and used to optimize the interpolation weights. At channel scale, different variogram models (e.g., spherical, Gaussian, exponential, and linear) were considered and the variograms which gave the best fit were chosen for the purpose of predicting K_v at each site. At watershed scale, different models using different sample sizes were fitted to linear variograms.

The performance of the spatial interpolation models were evaluated with cross validation which can be considered an objective method of assessing the quality of a variogram, or to compare the relative quality of two or more candidate variograms. To determine the goodness-of-fit for the variograms, the two most consistently useful statistics are: the median absolute deviation of the cross-validation residuals (MADXV) and the standard deviation of the cross-validation residuals (SDXV).

3 Results and discussions

3.1 Vertical streambed K_v

The mean K_v value varied from 8.37×10^{-3} to 8.51 m/day, about four orders of magnitude variation, indicating different types of soils with various structures across different stream orders. Stream gauge varied from 0.20 to 0.63 m while stream flow varied from 0.10 to 0.67 $m^3\ s^{-1}$ across the 10 sites, calculated from the USGS gauge data at Palisade and the watershed area above each reach. The summary statistics of streambed K_v values and hydrological conditions at each of the 10 test sites (stream channels) are shown in Table 1.

The K_v values in Spring Creek (Site 1) and Stinking Water Creek (Sites 2 and 3) were low ($<4.78 \times 10^{-2}$ m/d) and consistent with a silt and clay streambed according to the grain size analysis of core samples (Figure 4). The low values are due to a large amount of small-size particles (silt and clay) that filled the pore space of the coarser sand particles. Conversely, the sites in the Frenchman Creek channel (Sites 4–10) had higher K_v values because they consisted primarily of sand which has higher hydraulic conductivity than silt or clay.

Table 1 Summary statistics of K_v (m/day) values and hydrological conditions at 10 sites

Site	Channel shape	Sample size, n	Mean	Geometric mean	Minimum	Maximum	CV	Skewness	Kurtosis	Stream stage (m)	Streamflow ($m^3\ s^{-1}$)
1	S	9	8.37×10^{-3}	7.57×10^{-3}	3.88×10^{-3}	1.64×10^{-2}	0.49	1.02	0.51	0.37	0.27
2	S	9	1.67×10^{-2}	1.25×10^{-2}	6.11×10^{-3}	4.81×10^{-2}	0.91	1.59	1.31	0.31	0.10
3	S	9	4.78×10^{-2}	4.04×10^{-2}	1.01×10^{-2}	0.11	0.58	1.07	1.79	0.23	0.38
4	M	9	4.22×10^{-2}	2.23×10^{-2}	4.87×10^{-3}	0.19	1.36	2.49	6.71	0.28	0.29
5	M	9	0.25	0.10	4.48×10^{-3}	0.78	1.11	0.91	−0.54	0.63	0.32
6	M	12	0.27	0.16	3.03×10^{-2}	1.13	1.12	2.27	6.03	0.46	0.32
7	M	9	0.14	8.66×10^{-2}	5.65×10^{-3}	0.45	0.96	1.66	2.84	0.27	0.34
8	M	9	8.51	0.62	3.28×10^{-3}	26.8	1.32	0.86	−1.36	0.20	0.36
9	SC	9	8.02	1.42	1.54×10^{-2}	51.8	2.06	2.91	8.60	0.46	0.65
10	M	9	3.50	1.81	5.55×10^{-2}	9.04	0.96	1.02	−0.39	0.43	0.67

Abbreviations: CV, coefficient of variation; M, meandering (or curved) channel; S, straight channel; SC, slightly curved channel.

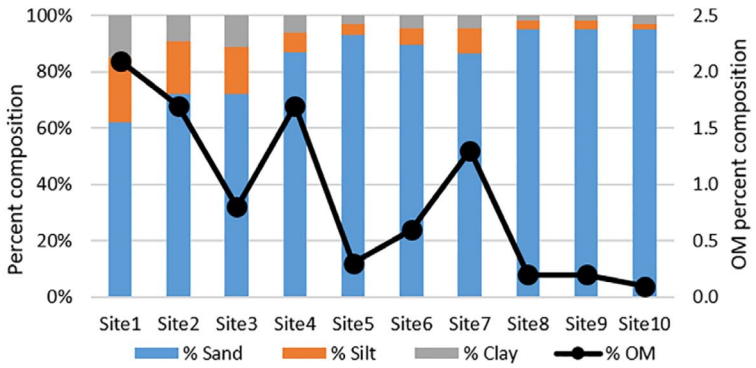

Figure 4 Soil textural compositions based on sieve analysis of 30 cm soil cores from the center permeameters in the middle transects at the 10 sites. Core recovery was typically greater than 95%. OM is the organic matter.

Meandering channels showed a more heterogeneous distribution of streambed K_v when compared to straight channels as shown by the higher coefficients of variation (Table 1). This difference in average K_v values shows that morphologic changes in meandering reaches caused changes in the streambed leading to erosion and deposition of sediments (Song et al., 2017; Zhang et al., 2017). For meandering stream channels, higher streambed K_v values were observed at the erosional outer bends and the middle of the channels than at the depositional inner bends due to the differences in particle size (Table 2). As a result of morphologic changes in meandering reaches, relatively larger particles were observed at the erosional channel banks, and the lower streambed K_v observed at the depositional channel banks can be attributed to finer particles that can cause streambed sediment

Table 2 Summary statistics of average K_v (m/day) values at meandering sites

Site	Channel shape	Erosional outer bend and middle of channel	Depositional inner bend
4	M	0.05	0.02
5	M	0.35	0.05
6	M	0.35	0.12
7	M	0.16	0.10
8	M	9.29	6.94
9	SC	11.82	0.43
10	M	4.27	1.96

Abbreviations: M, meandering (or curved) channel; SC, slightly curved channel.

clogging (Song et al., 2017). Moreover, even though our study was carried out in losing streams, higher streambed K_v were observed near the apex of reach bends. This agrees with the findings of Zhang et al. (2017) who observed that higher vertical water exchange fluxes significantly occurred near the apex of bends of gaining streams. Although streambed K_v along any side (left or right bank) of meandering channels showed some heterogeneity, in general, higher spatial variability was observed across stream channels than along stream channels.

3.2 Statistical distribution of streambed K_v

Owing to the fact that there are contradicting results as to which test is the optimal or best test (Yap & Sim, 2011), the aforementioned six normality tests were compared in order to see how they performed for both non-transformed and log-transformed K_v values at the 10 sites (Tables 3 and 4). A *p*-value less than .05 implies nonnormality of a distribution. The Q–Q plots for all combined log-transformed K_v values are shown in Figure 5. For each Q–Q plot, since both sets of quantiles come from the same distribution, the points form a fairly straight line, thus indicating that both sets of quantiles come from normal distributions.

Table 3 Test for normality for non-transformed K_v values (*p*-value)

Site no.	Anderson–Darling	Cramer–von Mises	Lilliefors (Kolmogorov–Smirnov)	Pearson chi-square	Shapiro–Francia	Shapiro–Wilk
1	0.38	0.39	0.54	0.26	0.32	0.35
2	0.00*	0.00*	0.00*	0.00*	0.01*	0.00*
3	0.19	0.21	0.37	0.05	0.15	0.27
4	0.00*	0.00*	0.02*	0.01*	0.00*	0.00*
5	0.06	0.07	0.21	0.05	0.08	0.06
6	0.01*	0.01*	0.07	0.05	0.00*	0.00*
7	0.05	0.05	0.02*	0.15	0.03*	0.04*
8	0.00*	0.00*	0.02*	0.00*	0.01*	0.01*
9	0.00*	0.00*	0.00*	0.00*	0.00*	0.00*
10	0.06	0.08	0.12	0.15	0.07	0.06

**p*-Value less than .05 implies non-normality of distribution.

Table 4 Test for normality for log-transformed K_v values (*p*-value)

Site no.	Anderson–Darling	Cramer–von Mises	Lilliefors (Kolmogorov–Smirnov)	Pearson chi-square	Shapiro–Francia	Shapiro–Wilk
1	0.95	0.98	1.00	0.80	0.99	0.93
2	0.07	0.07	0.04*	0.09	0.08	0.06
3	0.23	0.24	0.12	0.26	0.18	0.34
4	0.77	0.82	0.84	0.26	0.79	0.75
5	0.47	0.47	0.74	0.46	0.55	0.46
6	0.91	0.89	0.93	0.34	0.96	0.96
7	0.24	0.28	0.33	0.46	0.15	0.28
8	0.20	0.26	0.62	0.15	0.23	0.14
9	0.05	0.03*	0.05	0.02*	0.09	0.12
10	0.19	0.27	0.28	0.46	0.09	0.13

**p* Value less than .05 implies non-normality of distribution.

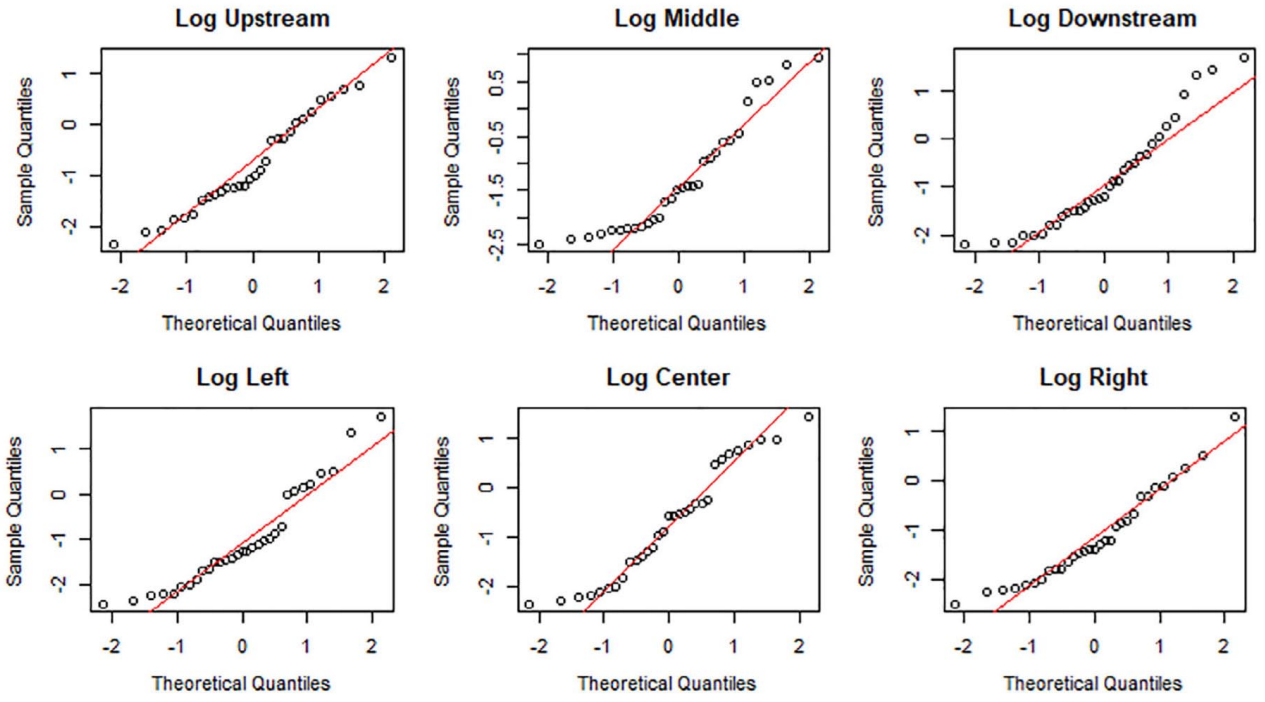

Figure 5 Q–Q plots of all streambed K_v values. *Top*: Log-transformed values for all upstream, middle and downstream transects; *Bottom*: Log-transformed values for all left, center, and right permeameters.

Table 5 Geostatistical summary of K_v (m/day) at 10 sites

Site	Model	MADXV	SDXV
1	Gaussian	0.0016	0.0045
2	Linear	0.0024	0.0111
3	Gaussian	0.0197	0.0322
4	Spherical	0.0109	0.0774
5	Linear	0.1309	0.3176
6	Exponential	0.1116	0.3744
7	Spherical	0.0522	0.1564
8	Linear	2.6062	11.893
9	Exponential	1.9349	18.594
10	Gaussian	1.5081	3.3649

3.3 Spatial distribution of streambed K_v

The goodness-of-fit statistics for the best variogram models for predicting streambed K_v at the 10 sites (channels) are presented in Table 5. For a heterogeneous aquifer, the effective hydraulic conductivity is known to be the geometric mean since samples of hydraulic conductivity in most cases follow a lognormal distribution (Dagan, 1981; Desbarats & Srivastava, 1991; Gómez-Hernández & Gorelick, 1989; Madden, 1976; Warren & Price, 1961). Since the *p*-values from at least four of the six tests are greater than .05 for all the 10 sites (Table 4), it can be stated with 95% confidence that the K_v data for the sites tended to follow a lognormal distribution. The spatial structure of the 10 geometric means (one value for each site) was also analysed and a linear variogram was fit to the data. In addition, 10 K_v values from middle transects and center permeameters were also used in gridding. Table 6 shows the nugget effect which is a reflection of measurement errors and variations that occur over distances smaller than the spacing of permeameter tests. The nugget effect was highest when all 93 tests were used (2.77) due to its highest variability of K_v values as indicated by its standard deviation and the coefficient of variation.

Results in Table 6 also show that the goodness-of-fit statistics are better when the geometric means for the 10 sites are used instead of all 93 K_v values. This is because the geometric mean gives a better summary of values at each site. When all values are used, there are a

Table 6 Statistics, parameters, and cross-validation goodness of- fit for linear variograms using different sample sizes

	N = **93***	N = **10****	N = **10*****
Standard deviation	6.80	0.66	3.33
Coeff. of variation	3.36	1.54	1.98
Nugget effect	2.77	2.156E-02	0
Anisotropy angle	30.8°	37.9°	38.1°
Variogram slope	8.75E-05	1.53E-06	8.818E-05
MADXV	0.18	0.08	0.16
SDXV	7.21	0.26	0.87

* Statistics calculated using all permeameter tests.
** Statistics calculated using the geometric means of the 10 sites.
*** Statistics calculated using the values from middle transects and center permeameters.

few extreme K_v values that tend to affect spatial interpolation, leading to negative K_v values downstream (Figure 6a). Negative K_v are due to Site 9 having the highest heterogeneity (0.015–51.8 m/d), coefficient of variation and skewness of the 10 sites (Table 1). This supports the argument that using the 93 K_v values directly (without using geometric mean per site) can lead to spatial interpolation errors. Furthermore, using only 10 values from the middle transects and center permeameters gives MADXV value of 0.16 which is similar to the MADXV estimated when all 93 K_v values are used (MADXV = 0.18 m/d) although the SDXV value of 0.87 m/d is much lower than 7.2 m/d.

The resulting contours are plotted using non-transformed K_v values gridded as linear (Figure 6a–d). Since using geometric means produced the best grid, log-transformed K_v values were also gridded as linear (Figure 6c). It is important to note that the contours do not start from the headwater subwatersheds because, at the time of study, the channels of the headwater subwatersheds were dry. Thus, extrapolation beyond the range of the data was treated sceptically since it was based on untestable assumptions about the behaviour of the data beyond their observed support, and there were no points around to constrain the models. Future work will focus on using a different approach for K_v (or saturated hydraulic conductivity, K_{sat}) estimation in dry streambeds. This will be significant for sites in headwater subwatersheds where streams are normally dry but recharge the groundwater system seasonally or intermittently.

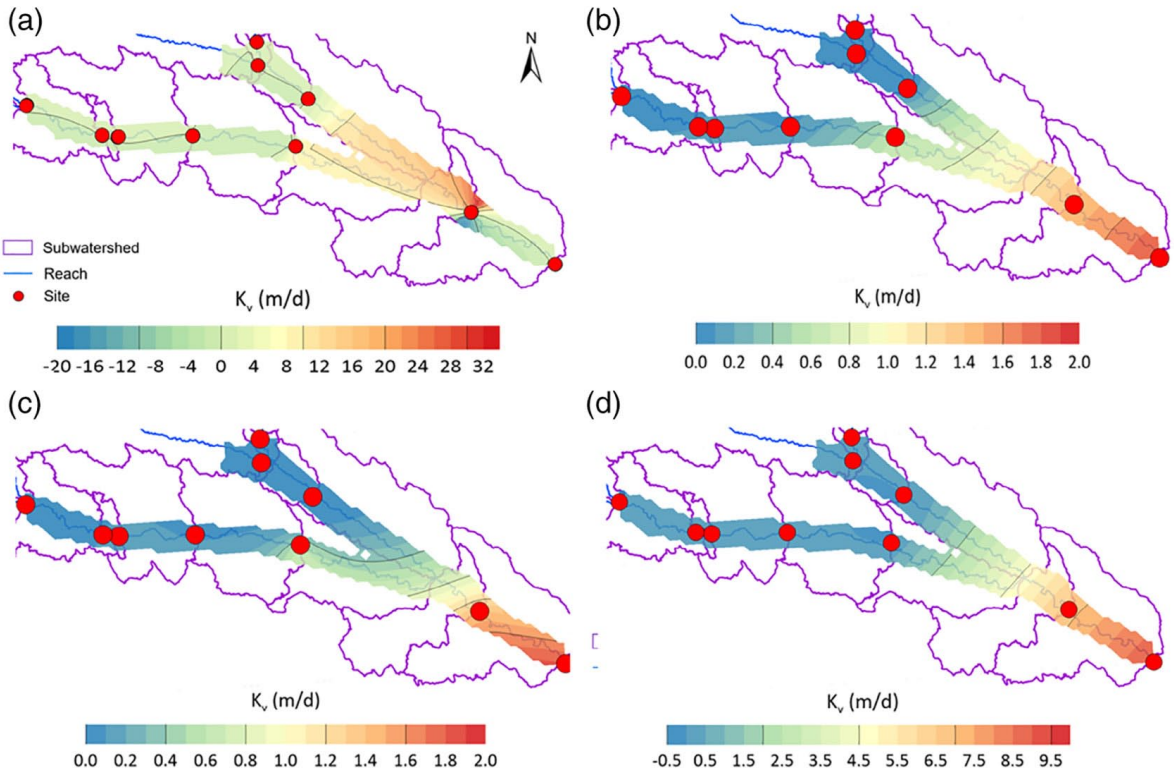

Figure 6 Spatial pattern based on (a) all 93 permeameters at the 10 sites using non-transformed values; (b) 10 geometric means using non-transformed values; (c) 10 geometric means using log-transformed values; (d) 10 values from center permeameters in the middle transects using non-transformed values. The boundary of spatial interpolation has been increased for better visualization of contour lines.

Figure 6b, c shows the similarity between the contours for non-transformed and log-transformed geometric mean values when both are gridded as linear. Although using 10 K_v values from center permeameters in the middle transects for gridding produced a relatively similar spatial pattern (Figure 6d) when compared to using geometric means (Figure 6b,c), there tends to be an over-prediction of K_v values across the watershed. This is because of the higher SDXV value of 0.87 m/d when compared to a value of 0.26 m/d (Table 6).

3.4 Effect of sedimentation processes on spatial distribution of K_v

In order to better understand the sedimentation processes, this study used the SSURGO database which consists of information about soil as collected by the National Cooperative Soil Survey over the

course of a century (USDA-NRCS, 2018) in the Unites States. We extracted the textural data (i.e., organic matter, sand, silt, and clay contents) and erodibility index for each county covered by the Frenchman Creek Watershed in Nebraska and Colorado (Figure 7; Abimbola et al., 2020). Although sieve analysis (Figure 4) of permeameter cores show that the streambed is mostly sandy (>95%) in the downstream areas with higher K_v values, the spatial distributions of the texture of topsoil (0–50 cm) show that there is about twice more silt than sand in the downstream areas (Sites 9 and 10) of the watershed compared to the upland areas (Figure 7). The higher K_v values in downstream areas is a result of downstream transition which occurs in stream channels as a result of the assortment of sediments coming from all points in a subwatershed or watershed and the spatial variation of soil textural properties of the sediment. Moreover, the sediment source of the tributaries plays a major role in controlling the grain-size distribution for streambed sediments (Singer, 2008).

In various applications of distributed hydrological models, spatial interpolation results of K_v can be useful in hydrological modelling using tools such as Soil and Water Assessment Tool (SWAT) and MODFLOW. Instead of assuming homogeneity of streambed K_v across a watershed, using grid results as input will help in calibrating this important parameter at reach or sub-watershed scale. Consequently, this will reduce prediction uncertainty and improve hydrological modelling results.

4 Conclusions

Spatial variability in the magnitudes and spatial patterns of streambed K_v will enhance the understanding of water and solute fluxes between groundwater and surface water in different morphologies, thus reducing uncertainties on streamflow prediction.

Although streambed K_v along any side (left or right bank) of meandering channels showed some heterogeneity, in general, higher spatial variability was observed across stream channels than along stream channels. Higher streambed K_v values were observed at the erosional outer bends and the middle of the channels than at the depositional inner bends. Also, higher streambed K_v was observed near the apex of reach bends.

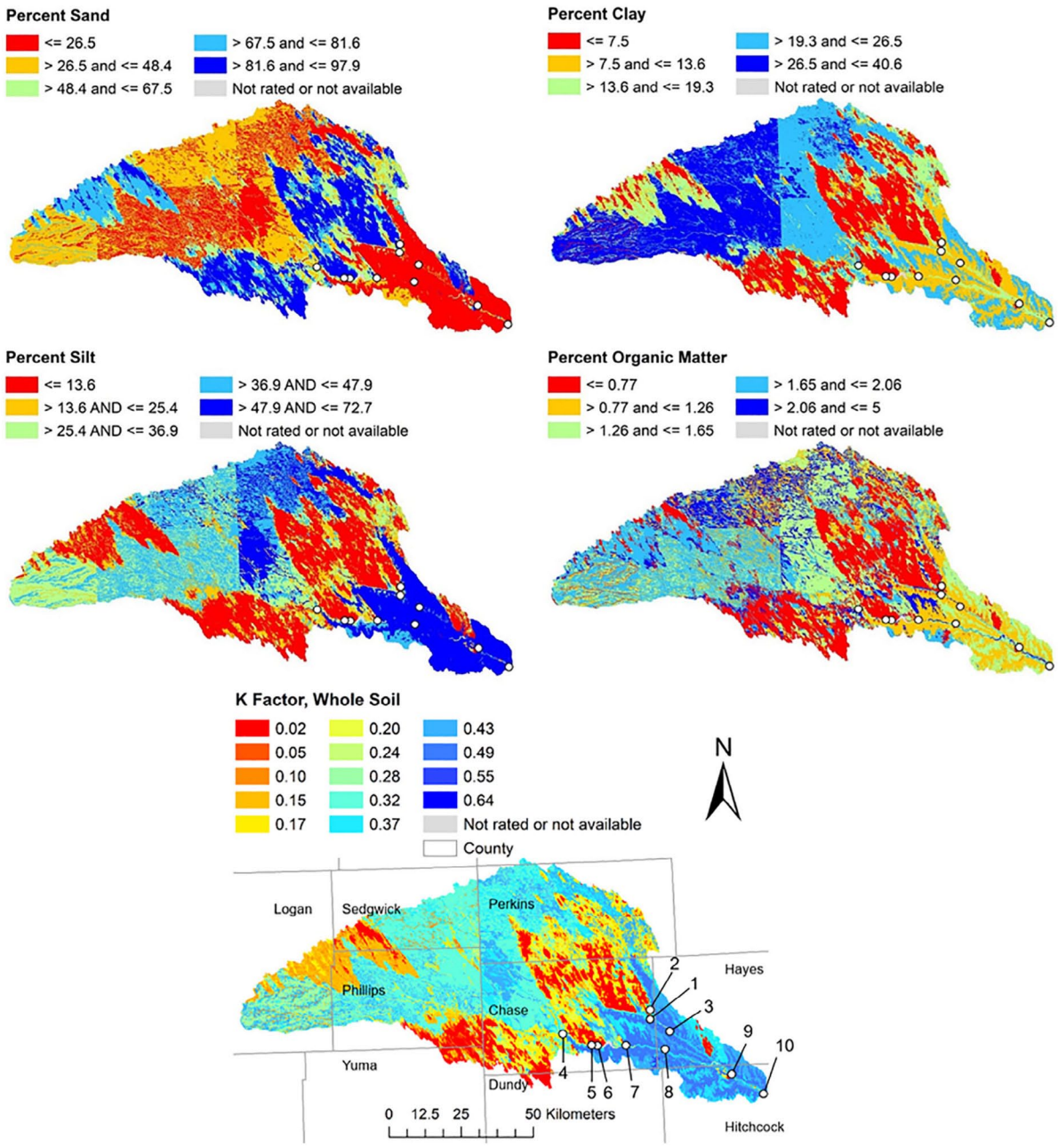

Figure 7 Spatial distributions of the soil properties for 0–50 cm depth. The sharp vertical and horizontal boundaries between classes in some maps are county boundaries which are effects of differences in how county soil surveys were conducted.

Geostatistical analysis shows that using the geometric means of the 10 sites performs better than using either all the K_v values from the 93 permeameter tests or 10 K_v values from the middle transects and center permeameters. In general, understanding the spatial variability of K_v and the uncertainty involved in both measurement and gridding is crucial to accurately predicting how stresses and environmental signals propagate through the hydrologic system. Grid results can be useful in calibrating streambed K_v at reach or sub-watershed scale in distributed hydrological models.

Future work will focus on using a different approach for K_v (or saturated hydraulic conductivity, K_{sat}) estimation in dry streambeds. This will be significant for sites in headwater subwatersheds where streams are normally dry but recharge the groundwater system seasonally or intermittently. More work is also needed to understand the spatio-temporal variations in streambed K_v across various natural systems, and to develop fast and accurate methods that will allow the surveying and gridding of larger watersheds, and also allow the representation of the dynamic behaviour of streambed K_v in distributed hydrological models.

Acknowledgments — The authors thank the U.S. Department of Agriculture - National Institute of Food and Agriculture (Hatch project NEB-21-177) as well as U.S. Geological Survey 104b Program for the support. The authors thank Jacob Rix and Martin Wells for assistance with sample collection and analysis.

Data availability — The data that support the findings of this study are available from the corresponding author upon reasonable request.

References

Abimbola, O. P., Mittelstet, A. R., Gilmore, T. E., & Korus, J. (2020). Influence of watershed characteristics on streambed hydraulic conductivity across multiple stream orders. *Scientific Reports*, *10*(1), 1–10.

Brunner, P., Cook, P. G., & Simmons, C. T. (2009). Hydrogeologic controls on disconnection between surface water and groundwater. *Water Resources Research*, *45*, W01422.

Burrough, P. A., & McDonnell, R. A. (1998). Optimal interpolation using geostatistics. In P. A. Burrough & R. A. McDonnell (Eds.), *Principles of geographical information systems* (pp. 132–161). Oxford, England: Oxford University Press.

Cardenas, M. B., & Zlotnik, V. A. (2003). A simple constant-head injection test for streambed hydraulic conductivity estimation. *Ground Water*, *41*(6), 867–871.

Castro, N. M., & Hornberger, G. M. (1991). Surface-subsurface water interactions in an alluviated mountain stream channel. *Water Resources Research*, *27*, 1613–1621.

Chen, X., & Shu, L. (2002). Stream-aquifer interactions: Evaluations of depletion volume and residual effects from groundwater pumping. *Ground Water*, *40*, 284–290.

Chen, X. H. (2000). Measurement of streambed hydraulic conductivity and its anisotropy. *Environmental Geology*, *39*(12), 1317–1324.

Chen, X. H. (2004). Streambed hydraulic conductivity for rivers in south- Central Nebraska. *Journal of the American Water Resources Association*, *40*(3), 561–574.

Chen, X. H. (2005). Statistical and geostatistical features of streambed hydraulic conductivities in the Platte River, Nebraska. *Environmental Geology*, *48*(6), 693–701.

Chen, X. H. (2007). Hydrologic connections of a stream-aquifervegetation zone in south-Central Platte River valley, Nebraska. *Journal of Hydrology*, *333*, 554–568. https://doi.org/10.1016/j.jhydrol.2006.09.020

Cheng, C., Song, J., Chen, X., & Wang, D. (2011). Statistical distribution of streambed vertical hydraulic conductivity along the Platte River, Nebraska. *Water Resource Management*, *25*, 265–285.

D'Agostino, R. B., & Stephens, M. A. (1986). *Goodness-of-fit techniques*. New York, NY: Marcel Dekker.

Dagan, G. (1981). Analysis of flow through heterogeneous random aquifers by the method of embedding matrix: 1. Steady flow. *Water Resource Research*, *17*(1), 107–121.

Desbarats, A. J., & Srivastava, R. M. (1991). Geostatistical characterization of groundwater flow parameters in a simulated aquifer. *Water Resources Research*, *27*(5), 687–698.

Dong, W. H., Chen, X. H., Wang, Z. W., Ou, G. X., & Liu, C. (2012). Comparison of vertical hydraulic conductivity in a streambed-sand bar system of a gaining stream. *Journal of Hydrology*, *450–451*, 9–16.

Genereux, D. P., Leahy, S., Mitasova, H., Kennedy, C. D., & Corbett, D. R. (2008). Spatial and temporal variability of streambed hydraulic conductivity in West Bear Creek, North Carolina, USA. *Journal of Hydrology*, *358*(3–4), 332–353.

Gómez-Hernández, J. J., & Gorelick, S. M. (1989). Effective groundwater model parameter values: Influence of spatial variability of hydraulic conductivity, leakance, and recharge. *Water Resources Research*, *25*(3), 405–419.

Goswami, D., Kalita, P. K., & Mehnert, E. (2010). Modeling and simulation of baseflow to drainage ditches during low-flow periods. *Water Resources Management*, *24*, 173–191.

Hatch, C., Fisher, A., Ruehl, C., & Stemler, G. (2010). Spatial and temporal variations in streambed hydraulic conductivity quantified with timeseries thermal methods. *Journal of Hydrology*, *389*, 276–288.

Hvorslev, M. J. (1951). *Time lag and soil permeability in groundwater observations*. Bulletin No. 36 (US Army Corps Eng.).

Irvine, D. J., Brunner, P., Franssen, H. H., & Simmons, C. T. (2012). Heterogeneous or homogeneous? Implications of simplifying heterogeneous streambeds in models of losing streams. *Journal of Hydrology*, *424–425*, 16–23.

Jiang, W. W., Song, J. X., Zhang, J. L., Wang, Y. Y., Zhang, N., Zhang, X. H., … Yang, X. G. (2015). Spatial variability of streambed vertical hydraulic conductivity and its relation to distinctive stream morphologies in the Beiluo River, Shaanxi Province, China. *Hydrogeology Journal*, *23*, 1617–1626. https://doi.org/10.1007/s10040-015-1288-4

Katsuyama, M., Tani, M., & Nishimoto, S. (2010). Connection between stream water mean residence time and bedrock groundwater recharge/discharge dynamics in weathered granite catchments. *Hydrological Processes*, *24*, 2287–2299.

Kennedy, C. D., Genereux, D. P., Mitasova, H., Corbett, D. R., & Leahy, S. (2008). Effect of sampling density and design on estimation of streambed attributes. *Journal of Hydrology*, *355*(1–4), 164–180.

Kurtz, W., Hendricks Franssen, H. J., Brunner, P., & Vereecken, H. (2013). Is high-resolution inverse characterization of heterogeneous river bed hydraulic conductivities needed and possible? *Hydrology and Earth System Sciences*, *17*, 3795–3813.

Leake, S.A., Greer, W., Watt, D., & Weghorst, P. (2008). *Use of superposition models to simulate possible depletion of Colorado River water by groundwater withdrawal*. USGS, Scientific Investigations Report 2008-5189; U.S. Geological Survey (USGS), Reston, VA.

Lilliefors, H. W. (1967). On the Kolmogorov–Smirnov test for normality with mean and variance unknown. *Journal of the American Statistical Association*, *62*, 534–544.

Madden, T. R. (1976). Random networks and mixing laws. *Geophysics*, *41*(6A), 1104–1125.

Naganna, S. R., Deka, P. C., Sudheer, C., & Hansen, W. F. (2017). Factors influencing streambed hydraulic conductivity and their implications on stream–aquifer interaction: A conceptual review. *Environmental Science and Pollution Research*, *24*, 24765–24789.

Royston, J. P. (1982). An extension of Shapiro and Wilk's W test for normality to large samples. *Applied Statistics*, *31*, 115–124.

Saenger, N., Kitanidis, P. K., & Street, R. L. (2005). A numerical study of surface-subsurface exchange processes at a riffle-pool pair in the Lahn River. *Germany. Water Resource Research*, *41*, W12424.

Shapiro, S. S., & Wilk, M. B. (1965). An analysis of variance test for normality (complete samples). *Biometrika*, *52*, 591–611.

Singer, M. B. (2008). Downstream patterns of bed material grain size in a large, lowland alluvial river subject to low sediment supply. *Water Resource Research*, *44*, W12202. https://doi.org/10.1029/2008WR007183.

Song, J., Chen, X., Cheng, C., Summerside, S., & Wen, F. (2007). Effects of hyporheic processes on streambed vertical hydraulic conductivity in three rivers of Nebraska. *Geophysical Research Letters*, *34*, L07409.

Song, J., Wang, L., Dou, X., Wang, F., Guo, H., Zhang, J., … Zhang, B. (2018). Spatial and depth variability of streambed vertical hydraulic conductivity under the regional flow regimes. *Hydrological Procedure*, *32*(19), 3006–3018.

Song, J., Zhang, G., Wang, W., Liu, Q., Jiang, W., Guo, W., … Dou, X. (2017). Variability in the vertical hyporheic water exchange affected by hydraulic conductivity and river morphology at a natural confluent meander bend. *Hydrological Procedure*, *31*(19), 3407–3420.

Sun, D., & Zhan, H. (2007). Pumping induced depletion from two streams. *Advances in Water Resources*, *30*, 1016–1026.

Traylor, J. P. (2012). *Analytical modeling of irrigation and land use effects on streamflow in semi-arid conditions: Frenchman Creek, Nebraska* (MSc thesis), University Nebraska-Lincoln, Lincoln, NE.

Twidwell, D., Rogers, W. E., Fuhlendorf, S. D., Wonkka, C. L., Engle, D. M., Weir, J. R., … Taylor, C. A., Jr. (2013). The rising Great Plains fire campaign: citizenry response to woody plant encroachment. *Frontiers in Ecology & Environment*, *11*(1), e64–e71.

USDA-NRCS. (2018). Description of SSURGO Database. Natural Resources Conservation Service, United States Department of Agriculture. Web Soil Survey. Retrieved from https://websoilsurvey.nrcs.usda.gov/

Wang, L., Jiang, W., Song, J., Dou, X., Guo, H., Xu, S., … Li, Q. (2017). Investigating spatial variability of vertical water fluxes through the streambed in distinctive stream morphologies using temperature and head data. *Hydrogeology Journal*, *25*, 1283–1299. https://doi.org/10.1007/s10040-017-1539-7

Wang, W., Lu, H., Yang, D., Sothea, K., Jiao, Y., Gao, B., … Pang, Z. (2016). Modelling hydrologic processes in the Mekong River Basin using a distributed model driven by satellite precipitation and rain gauge observations. *PLoS One*, *11*(3), e0152229 https://doi.org/10.1371/journal.pone.0152229

Warren, J. E., & Price, H. S. (1961). Flow in heterogeneous porous media. *Society of Petroleum Engineers Journal*, *1*, 153–169.

Webster, R., & Oliver, M. (2001). *Geostatistics for environmental scientists*. Chichester, England: Wiley.

Woessner, W. W. (2000). Stream and fluvial plain ground water interactions: Rescaling hydrogeologic thought. *Ground Water*, *38*(3), 423–429.

Yap, B. W., & Sim, C. H. (2011). Comparisons of various types of normality tests. *Journal of Statistical Computation and Simulation*, *81*(12), 2141–2155. https://doi.org/10.1080/00949655.2010.520163

Zhang, G., Song, J., Wen, M., Zhang, J., Jiang, W., Wang, L., … Wang, Y. (2017). Effect of bank curvatures on hyporheic water exchange at meter scale. *Hydrology Research*, *48*(2), 355–369.